Journal of Additive Manufacturing Technologies
DOI: 10.18416/JAMTECH.2111531

Infinite Science | Publishing

Surface texture and high cycle fatigue of as-built metal additive AlSi7Mg0.6

T. Buchenau[1*], M. Amkreutz[1], and H. Bruening[1]

[1] *Fraunhofer Institute for Manufacturing Technology and Advanced Materials IFAM, Bremen, Germany*
[*] *Corresponding author, email: theresa.buchenau@ifam.fraunhofer.de*

Abstract

The aluminium silicon alloy AlSi7Mg0.6 is gaining importance in additive manufacturing. This work is showing a correlation of surface quality and fatigue properties of three different AlSi7Mg0.6 as-built surfaces manufactured by laser powder bed fusion. All specimens were built in z-direction and the difference in surface quality was achieved by variation of the contour scanning parameters in the manufacturing process.

Focus of the evaluation is on the reduced valley depth Svk rather than the commonly applied Ra (arithmetic mean of the line roughness profile) and Rt (maximum total height of the line roughness profile) and their areal equivalents Sa and Sz. Svk is derived from the material ratio curve and is a measure of the size of the valley population across the sample. It was found to show a better correlation with number of cycles to failure than parameters based on local extreme values such as Sz and Sv (depth of deepest detected valley).

Keywords: Laser powder bed fusion, Optical surface texture measurement, Additive manufacturing, Fatigue, AlSi7Mg0.6

1. Introduction

Additive manufacturing (AM) technologies enable geometrical freedom, material savings and functional integration unimaginable with conventional subtractive methods. Laser powder bed fusion (LPBF) is one of the most commonly used additive manufacturing technologies. Typical surface features of as-built LPBF surfaces are powder particle agglomerations and re-entrant features, leading to a high initial surface roughness, which is associated with poor fatigue performance [1].

In recent years, aluminium alloys are increasingly used in AM due to their applications in the automotive and aerospace industries. The interest in AlSi7Mg0.6 specifically has been growing as it has good corrosion resistance, weldability and mechanical properties [2].

1.1. Surface characterization for metal AM

Surface texture is often described by means of the ISO 4287 parameters Ra (arithmetic mean of the line roughness profile) and Rt (maximum total height of the line roughness profile), determined by use of contact stylus measurements [3]. Both, parameters and metrology, are established and still widely used in industry and literature and likewise for metal AM surface texture characterization [4-10, 21].

While the areal equivalents to those commonly used parameters, Sa and Sz, at least offer a more statistically significant representation of the evaluated surface as compared to line roughness, Sa and Sz are still sensitive to local extreme values and are certainly not the best fit when a description of overall surface quality is required. Literature shows investigations on various ISO 25178 parameters, such as Sa, Sz, Sv (deepest valley depth) or Ssk (shift of height distribution below or above mean plane, equal to zero for symmetrical distribution) [11, 12] and feature based approaches [13].

In this work, parameters derived from the material ratio curve [14, 15], particularly the core height Sk, reduced valley depth Svk and lower profile portion Smr2, are applied as they offer a more robust description of the as-built LPBF surface condition [16].

1.2. Mechanical properties of AlSi7Mg0.6 from laser powder bed fusion

Ultimate tensile strength values for AlSi7Mg0.6 specimens manufactured in an LPBF process in vertical direction (layer-by-layer built-up perpendicular to the applied force in mechanical testing), vary between approximately 300 MPa [17] and over 400 MPa [2, 18, 19]. This means most of the values for as-built LPBF samples exceed the ultimate strength of the cast alloy with T6 heat treatment, which is between 320 and 360 MPa [19].

There are only a few studies on fatigue behaviour of the AlSi7Mg0.6 alloy. Some work on rotating bending fatigue with variation of LPBF contour scan parameters was done by Nasab et al. [20]. Bassoli et al. [17]

performed a full Wöhler curve characterization of one set of as-built specimens.

1.3 Objective

Numerous studies look into the correlation of surface texture and fatigue properties for metal AM parts, mostly utilizing common parameters such as Ra, Rz, Rt, Sa, Sz or Sv [7, 10, 21]. Literature mainly shows studies on different surface states obtained from post-processing [7] or from variation of build orientation [10]. However, the latter also affects the bulk properties of a tested sample, resulting in the assessment of a combined bulk and surface effect.

The fatigue specimens used in this work were manufactured with identical bulk parameters and build orientation, only varying the contour scan parameters to obtain differences in surface quality while maintaining bulk properties. By varying the contour scan speed, three different as-built surface conditions could be achieved and analyzed.

This work aims at showing the difference in mechanical performance under axial cyclic loading for three as-built LPBF surface conditions of AlSi7Mg0.6 specimens and correlation of fatigue life with alternative standardized parameters.

2. Material and methods

2.1. Evaluated samples

Three sets of samples of as-built surface condition exhibiting different surface quality and features were created, namely AsB – smooth, AsB – medium and AsB – rough. The manufacturing conditions on the Trumpf TruePrint 1000 LPBF system are given in Table 1. The manufacturing parameters only differ in the contour scan speed, the bulk parameters were identical. All samples had a density higher than 99%.

Table 1. AlSi7Mg0.6 manufacturing parameters on Trumpf TruePrint 1000.

Bulk	Layer thickness [µm]	30
	Hatch distance [mm]	0.12
	Laser power [W]	166
	Pre-sinter [-]	No
	Scan speed [mm/s]	1000
Contour (smooth/ medium/ rough)	Layer thickness [µm]	30
	Hatch distance [mm]	0.12
	Laser power [W]	195
	Pre-sinter [-]	Yes
	Scan speed [mm/s]	300 / 900 / 1200

The fatigue specimen geometry was developed in line with ASTM 466–15 with the following theoretical geometrical specifications: Total height 80 mm, smallest cross section width 6 mm, and thickness 3 mm. Fig. 1 shows a fatigue specimen after mechanical testing with indication of build direction.

Macroscopic and microscopic visual inspection of the samples confirm that they indeed show differences in surface quality. Differences in size and quantity of particle agglomerations can be seen in Fig. 2.

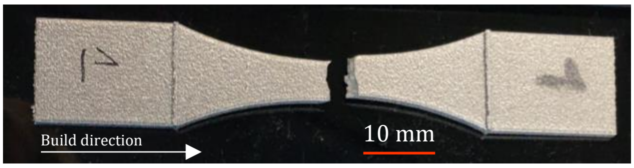

Fig 1. Fatigue specimen after mechanical testing.

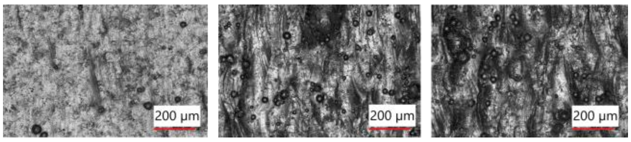

Fig 2. Microscopic images of evaluated surface conditions, showing particle agglomerations of different size and quantity: AsB – smooth (left), AsB – medium (middle) and AsB – rough (right).

2.2. Surface characterization

For the surface texture characterization the Keyence VR3200 fringe projection system was used at a lateral resolution of 3.7 µm. In the style of the ISO 4287 line parameters, ISO 25178 areal parameters were evaluated by averaging results from 5 individual areas, illustrated in Fig. 3.

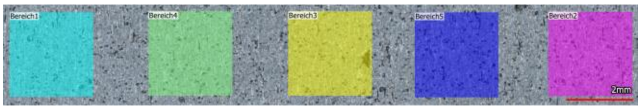

Fig 3. ISO 25178 parameter evaluation: Mean values of 5 individual square areas of 2.5 x 2.5 mm^2, similar to the ISO 4287 line roughness calculation.

The selected surface texture parameters are the commonly used areal parameters Sa (absolute mean height), Sq (root mean square height), Sz (maximum total height) and Sv (maximum valley depth), as well as the material ratio curve parameters Sk (core height) and Svk (reduced valley depth) and Smr2 (valley profile portion). Sk, Svk and Smr2 are illustrated in Fig. 4. Sk (spacing between red dashed lines) is determined from the intersection of the curve's main slope (light blue dashed line) with vertical lines at 0% and 100%. Svk represents the average valley depth below the core material. Smr2 marks the percentage above which the valley portion of the profile is depicted on the curve.

For more detailed information on the parameters briefly explained above, please refer to [14-16].

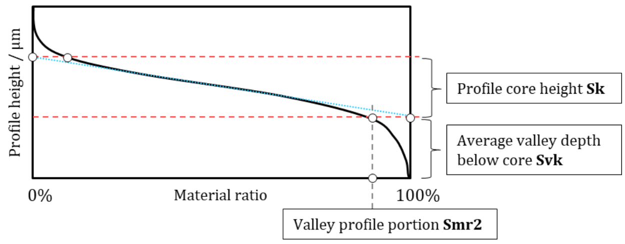

Fig 4. Material ratio curve, determination of Sk, Svk and Smr2.

Journal of Additive Manufacturing Technologies
DOI: 10.18416/JAMTECH.2111531

2.3. Mechanical Testing

Fatigue testing was performed on a DYNA-MESS 4S 20kN Z/D system at a frequency of 20 Hz and a stress ratio R = 0.1. The load levels were defined w.r.t. the ultimate strength acquired from tensile testing, σ_{ult} = 392 ± 5 MPa, corresponding values are specified in Table 2.

Table 2. Load levels and stress values for σ_{ult} = 392 MPa and R = 0.1.

Load level $\sigma_{max}/\sigma_{ult}$	σ_{max} / MPa	σ_{min} / MPa	σ_{mean} / MPa
0.4	156.8	15.7	86.2
0.5	196.0	19.6	107.8
0.6	235.2	23.5	129.4
0.7	274.4	27.4	150.9

3. Results and discussion

3.1. Surface characterization

Table 3 shows results of the commonly used parameters Sa, Sq, Sz and Sv and the material ratio curve parameters Sk, Svk and Smr2. For each set of samples, at least 9 specimens were included in the evaluation of mean and standard deviation values presented.

When grouping the parameters w.r.t. their contained information, Sa, Sq and Sk can be categorized as indicators for the overall surface quality as they are related to the mean profile height. Sz, Sv and Svk on the other hand, are measures for extreme values, while Sz and Sv are absolute maxima and Svk represents an average value of valley depths. Smr2 is the profile percentage marking the portion of the profile associated with valleys below the core material. It is believed, that this parameter has the potential to give an indication of the profile share critical for crack initiation. In this work, Svk is interpreted as a measure for the average size of potential crack initiation points present on the surface and is compared to Sv, the maximum valley depth, in particular concerning the correlation with fatigue properties.

Looking at the results presented in Table 3, the three considered as-built surface conditions can be clearly distinguished by all of the chosen surface texture parameters. The standard deviation is in the same order of magnitude for all mean/core height related parameters (Sa, Sq, Sk) between 3% and 7%. For Svk, the standard deviation is slightly higher (up to 10%), while it reaches between 8% and 28% for Sz and Sv. The large standard deviations for parameters representing extreme values across the profile make sense as they are strongly dependent on the measured location. This circumstance also results in the possibility of not detecting the deepest valleys. Smr2 values of around 90% for all of the as-built surface conditions suggest that 10% of the areal profile belong to the reduced valley portion. Svk values of 3.1, 6.0 and 8.3 µm for the smooth, medium and rough set, respectively, indicate the average depth of the corresponding valleys.

Table 3. Surface texture parameters for AsB – smooth, AsB – medium and AsB – rough, L-filter = 0.25 mm, S-filter = 8 µm, R^2_{adj} for Sz, Sv and Svk for exponential fit at 0.5*σ_{ult}.

		Sa / µm	Sq / µm	Sk / µm
AsB - smooth	*Mean*	2.58	3.36	7.89
	St.-dev.	0.161	0.221	0.490
	% St.-dev.	6	7	6
AsB - medium	*Mean*	4.74	6.05	14.96
	St.-dev.	0.173	0.259	0.527
	% St.-dev.	4	4	4
AsB - rough	*Mean*	5.99	8.14	17.37
	St.-dev.	0.222	0.314	0.558
	% St.-dev.	4	4	3

		Sz / µm	Sv / µm	Svk / µm	Smr2 / %
R^2_{adj} for 0.5*σ_{ult}		0.849	0.895	0.971	n/a
AsB - smooth	*Mean*	49.90	16.55	3.10	90.31
	St.-dev.	5.768	1.355	0.256	0.158
	% St.-dev.	12	8	8	0.2
AsB - medium	*Mean*	79.94	36.69	6.00	90.05
	St.-dev.	13.811	7.109	0.396	0.161
	% St.-dev.	17	19	7	0.2
AsB - rough	*Mean*	124.59	63.76	8.32	89.61
	St.-dev.	23.561	17.918	0.839	0.446
	% St.-dev.	19	28	10	0.5

3.2. Fatigue

The fatigue results for the three as-built surface conditions are presented in Fig. 5. The AsB – smooth samples clearly endure the highest number of cycles, AsB – medium and AsB – smooth results overlap at load level 0.6*σ_{ult}. The number of cycles to failure for the AsB – rough set of samples at load level 0.4*σ_{ult} and 0.5*σ_{ult} correspond with values determined by Bassoli et al., 2018. However, their study did not include surface quality of the tested specimens and was performed at R=0 [17].

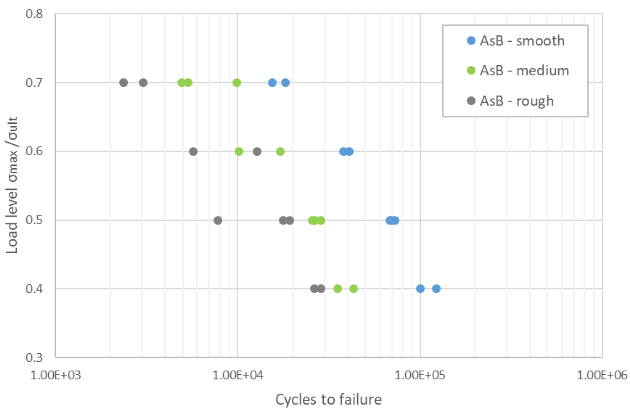

Fig 5. Fatigue results for three surface conditions at four load levels each. Load levels are specified i.t.o. σ_{ult}.

Looking at the fracture areas, it can be confirmed, that for the AsB - medium and AsB – rough specimens, all

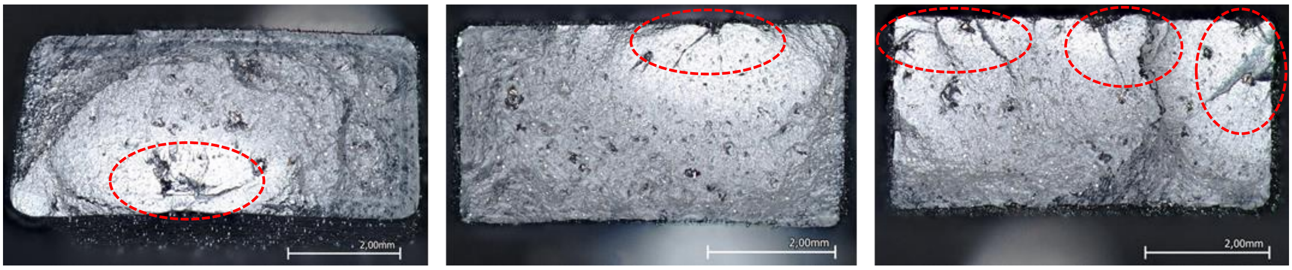

Fig 6a. AsB – smooth (left): Crack propagation from bulk defect, **b.** AsB – medium (middle): Surface crack causing fatigue failure, **c.** AsB – rough (right): Simultaneous crack initiation from multiple surface defects.

cracks started from the surface, in many cases even multiple crack initiation was observed, which is a common phenomenon for as-built AM surfaces [22]. 5 out of 10 AsB – medium specimens and 9 out of 9 AsB – rough specimens exhibited multiple crack initiation from the surface. Among the AsB – smooth specimens, only one case of multiple crack initiation from the surface was observed. 5 out of 9 fatigue failures started from individual surface cracks, 3 out of 9 started from bulk defects. Table 4 gives a summary of failure initiation for all evaluated specimens, Fig. 6a – 6c show examples of the different observed types of crack initiation.

Table 4. Crack initiation for specimens of the three evaluated surface conditions.

Surface condition	Total # of samples	Crack initiation type / # of samples	# multiple crack initiation
AsB - smooth	9	Surface / 6 Bulk / 3	1
AsB - medium	10	Surface / 10	5
AsB - rough	9	Surface / 9	9

The collected data confirms that AM surfaces with a higher roughness (i.e., higher density of partical agglomerations) are more likely to experience multiple crack initiation during cyclic loading, resulting in failure after a fewer number of cycles. Smoother as-built surfaces, such as AsB – smooth, appear to be less likely to experience multiple crack initiation.

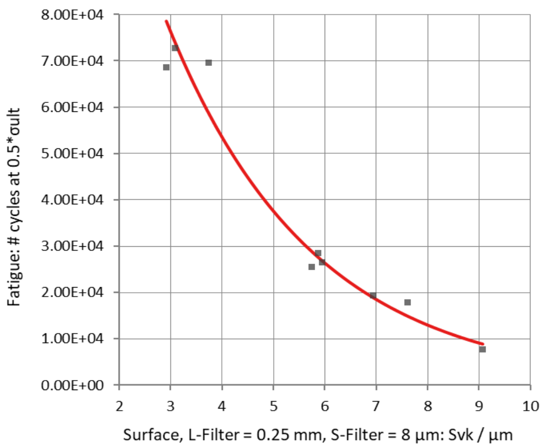

Fig. 7. Number of cycles vs. Svk [µm] for all surface conditions, exponential fit with R^2_{adj} = 0.971.

3.3. Fitting fatigue and surface quality data

When plotting data of all three surface conditions for individual load levels, an exponential function results in a good fit for the data. Fig. 7 and Fig. 8 show the number of cycles vs. Svk and Sv, respectively. Comparing both curves, it can be observed that the Svk fit (red line) is closer to the actual data points (grey squares) than for Sv, quantifiable by the respective R^2_{adj}-values of 0.971 (Svk) and 0.895 (Sv). Additionally, Table 3 contains the R^2_{adj}-value of Sz, equal to 0.849.

The curve for the number of cycles to failure (# cycles) as a function of Svk at a load level of $0.5*\sigma_{ult}$ is described by

$$\# \text{ cycles } (Svk) = 2.207 \cdot 10^5 \cdot 0.7016^{Svk} \qquad (1)$$

The presented results suggest that the Svk parameter gives a better correlation of the surface condition and fatigue behavior than Sv and Sz. Rather than only comprising information on individual extreme values, it provides information on the valley population across a sample. Especially when taking into account that multiple crack initiation from surface defects is a typical cause of failure for as-built AM parts, it seems reasonable to use Svk when correlating surface and fatigue properties. Also the combination with Smr2 might be worthwhile looking into.

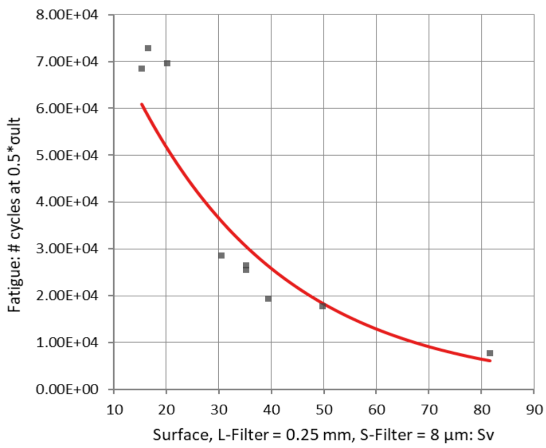

Fig. 8. Number of cycles vs. Sv [µm] for all surface conditions, exponential fit with R^2adj = 0.895.

4. Conclusions

At the current state of this research, the following conclusions can be drawn:

- The reduced valley depth Svk (derived from the material ratio curve) is more robust and reproducible than maximum valley depth Sv and maximum total profile height Sz.
- The fatigue behavior of as-built AlSi7Mg0.6 LPBF parts is strongly related to the surface quality. AsB – smooth specimens hardly experience multiple crack initiation while it is common for AsB – rough specimens.
- Rougher AM surfaces are associated with higher individual profile extreme values Sz and Sv, which are frequently applied when correlating surface quality and fatigue behavior. However, these surfaces are also likely to exhibit multiple crack initiation, justifying the shift toward using Svk, which characterizes the valley population present on the surface.
- Svk shows a better correlation than the more frequently used Sv with number of cycles to failure for the evaluated load levels and surface conditions.

In order to fully characterize the fatigue behavior of as-built LPBF AlSi7Mg0.6 parts, full Wöhler curve assessment, residual stress measurement and fatigue limit determination for all created surface conditions is ongoing. This will enable the application of existing models for the correlation of fatigue and defects to less commonly used surface texture parameters like Svk.

Acknowledgments

Thanks to Inga-Malena Meyenborg for manufacturing the samples, Annette Schwingen for performing tensile testing, Marc-Oliver Becker for his support with the fatigue testing equipment and Nicola Cersullo for sharing his expertise in metal fatigue.

Author's statement

Conflict of interest: Authors state no conflict of interest. Informed consent: Informed consent has been obtained from all individuals included in this study. Ethical approval: The research related to human use complies with all the relevant national regulations, institutional policies and was performed in accordance with the tenets of the Helsinki Declaration, and has been approved by the authors' institutional review board or equivalent committee.

References

1. Uriondo, A; Esperon-Miguez, M.; Perinpanayagam, S.: The present and future of additive manufacturing in the aerospace sector: A review of important aspects. *Proceedings of the Institution of Mechanical Engineers, Part G: Journal of Aerospace Engineering*, 229(11):2132-2147, 2015.
2. Mauduit, A.; Gransac, H.; Auguste, P.; Pillot, S.; Diószegi, A. (2019): Study of AlSi7Mg0.6 Alloy by Selective Laser Melting: Mechanical Properties, Microstructure, Heat Treatment. In: *jcme 3 (1)*, S. 1. DOI: 10.7494/jcme.2019.3.1.1.
3. ISO 4287: Geometric Product Specifications (GPS) - Surface texture: Profile method - Terms, definitions and surface texture parameters, 1997.
4. Townsend, A.; Senin, N.; Blunt, L.; Leach, R. K.; Taylor, J. S. (2016): Surface texture metrology for metal additive manufacturing: a review. In: *Precision Engineering 46*, S. 34–47. DOI: 10.1016/j.precisioneng.2016.06.001.
5. Triantaphyllou, A.; Giusca, C. L.; Macaulay, G. D.; Roerig, F.; Hoebel, M.; Leach, R. K. (2015): Surface texture measurement for additive manufacturing. In: *Surf. Topogr.: Metrol. Prop. 3 (2)*, S. 24002. DOI: 10.1088/2051-672X/3/2/024002.
6. Bagehorn, S.; Mertens, T.; Greitemeier, D.; Carton, L.;. Schoberth, A.: Surface finishing of additive manufactured Ti-6Al-4V - a comparison of electrochemical and mechanical treatments. In: *6th European Conference for Aerospace Sciences*, 06 2015.
7. Bagehorn, S.; Wehr, J.; Nixon, S.; Balastrier, A.; Mertens, T.; Maier, H.: Electrochemical Enhancement of the Surface Morphology and the Fatigue Performance of Ti-6Al-4V Parts Manufactured by Laser Beam Melting. In: *Solid Freeform Fabrication 2017*, 2017.
8. Calignano, F.; Manfredi, D.; Ambrosio, E.; Iuliano, L.; Fino. P.: Influence of process parameters on surface roughness of aluminum parts produced by DMLS. *The International Journal of Advanced Manufacturing Technology*, 67(9-12):2743-2751, 2013.
9. Krishna, A. V.: *Towards Topography Characterization of Additive Manufacturing Surfaces*. Licentiate engineering thesis, Chalmers University of Technology, Gothenburg, Sweden, 2020.
10. Nicoletto, G.; Konečná, R.; Frkáň, M.; Riva, E. (2018): Surface roughness and directional fatigue behavior of as-built EBM and DMLS Ti6Al4V. In: *International Journal of Fatigue 116*, S. 140–148. DOI: 10.1016/j.ijfatigue.2018.06.011.
11. Flys, O.; Berglund, J.; Rosen, B.-G. (2020): Using confocal fusion for measurement of metal AM surface texture. *Surface Topography: Metrology and Properties*, 8(2):024003, 2020.
12. Townsend, A.; Racasan, R.; Blunt, L. (2018): Surface-specific additive manufacturing test artefacts. In: *Surf. Topogr.: Metrol. Prop. 6 (2)*, S. 24007. DOI: 10.1088/2051-672X/aabcaf.
13. Senin, N.; Thompson, A.; Leach, R. (2018): Feature-based characterisation of signature topography in laser powder bed fusion of metals. *Measurement Science and Technology*, 29(4):045009.
14. Leach, R.: *Characterisation of Areal Surface Texture*. Springer Berlin Heidelberg, Berlin, Heidelberg, 2013.
15. ISO 25178: Geometric Product Specifications (GPS) - Surface texture: areal - Part 2: Terms, definitions and surface texture parameters, 2012.
16. Buchenau, T.; Amkreutz, M.; Brüning, H.; Norda, M. (2019): Evaluation of Alternative Parameters to Describe the Quality of Additively Manufactured Aluminium Alloy Surfaces. *Additive Manufacturing Conference Turkey 2019*. AMC Turkey Comittee. Istanbul, Turkey, 17.10.2019
17. Bassoli, E.; Denti, L.; Comin, A.; Sola, A.; Tognoli, E. Fatigue Behavior of As-Built L-PBF A357.0 Parts. *Metals* 2018, *8*, 634. https://doi.org/10.3390/met8080634
18. Grande, A. M.; Cacace, S.; Demir, A. G.; Sala, G. (2019): Fracture and fatigue behaviour of AlSi7Mg0,6 produced by Selective Laser Melting effects of thermal treatments. In: *25th International Congress, Italian Association of Aeronautics and Astronautics*.
19. Rao, J. H.; Zhang, Y.; Fang, X.; Chen, Y.; Wu, X.; Davies, C.H.J. (2017): The origins for tensile properties of selective laser melted aluminium alloy A357. *Additive*

Manufacturing 17, pp. 113–122. DOI: 10.1016/j.addma.2017.08.007.

20. Hamidi Nasab, Milad; Romano, Simone; Gastaldi, Dario; Beretta, Stefano; Vedani, Maurizio (2019): Combined effect of surface anomalies and volumetric defects on fatigue assessment of AlSi7Mg fabricated via laser powder bed fusion. *Additive Manufacturing*, p. 100918. DOI: 10.1016/j.addma.2019.100918.
21. Zerbst, U.; Bruno, G.; Buffière, J.-Y.; Wegener, T.; Niendorf, T.; Wu, T. et al. (2021): Damage tolerant design of additively manufactured metallic components subjected to cyclic loading: State of the art and challenges. In *Progress in Materials Science*, p. 100786. DOI: 10.1016/j.pmatsci.2021.100786.
22. Beretta, S.; Gargourimotlagh, M.; Foletti, S.; Du Plessis, A.; Riccio, M. (2020): Fatigue strength assessment of "as built" AlSi10Mg manufactured by SLM with different build orientations. In *International Journal of Fatigue* 139, p. 105737. DOI: 10.1016/j.ijfatigue.2020.105737.